Compressive residual stresses in thin sputtered amorphous carbon films

D. Wan and K. Komvopoulos

Department of Mechanical Engineering, University of California, Berkeley, CA 94720

Abstract

A large compressive residual stress occurs in sputtered amorphous carbon (a-C) films. Evaluation and relaxation of the compressive residual stresses in low-pressure radio-frequency (rf) sputtered a-C films were investigated by experiments, and explained in terms of the effects of Ar^+ bombardment, thermal spike, and interfacial tension. The stress level was essentially dependent of Ar^+ bombardment on the growing film surfaces, and can reach to a value as high as -10 GPa with intensive Ar^+ bombardment. The origin and development of the compressive residual stress were related to Ar^+ bombardment kinetic energy and ion flux. The compressive residual stress in rf sputtered a-C films relaxed due to thermal spike processes or interfacial tension effects.

I. INTRODUCTION

Large compressive residual stresses are usually produced in amorphous carbon (*a*-C) films deposited by low-pressure radio-frequency (rf) sputtering. The effect of compressive residual stresses on the tribological performance of *a*-C films deposited by magnetron sputtering as a protective coating has been studied experimentally (Mounier et al., 1995; Mounier et al., 1997). Severe damage and formation of wear debris were attributed to the high level of compressive residual stress in the *a*-C films. The residual stress effect on the tribological performance of thin films has also been examined in theoretical and numerical studies (Hills et al., 1982; Ye, 2002). Intense Ar^+ bombardment on the growing film surface controls the magnitude of the compressive stress. However, the relationship between Ar^+ bombardment and the compressive residual stress is complicated (Windischmann, 1992; Davis, 1993). Various theories have been proposed to explain the origin and magnitude of the residual stresses in thin films (Machlin, 1995). Numerous techniques have been used to measure the residual stress in thin films (Nix, 1989), such as X-ray diffraction, optical inteferometry, and laser scanning. However, these routine techniques may not be suitable for ultrathin films of thickness of the order of a few nanometers. Small amounts of Ar atoms implanted in the film as stress-sensing probes has been proposed to evaluate residual stresses in ultrathin films (Lu et al., 2000), which is based on the effect of the residual stress on the binding energy shift of Ar atoms.

Compressive residual stresses in rf sputtered *a*-C films deposited on Si(100) substrates under different conditions were systematically studied by experiments in this study. The residual stresses were determined by measuring the wafer curvature before and after film deposition. The effect of energetic ion bombardment on the residual stress and the stress relaxation mechanisms, such as

thermal spikes and interfacial tension effect, were discussed in the context of the obtained experimental results.

II EXPERIMENTAL PROCEDURES

Five groups of a-C films were deposited on 3-inch Si(100) wafers by Ar^+ sputtering of a pure graphite target using a Perkin-Elmer sputtering system without magnetron. The vacuum chamber was first pumped down to a low base pressure ($< 2 \times 10^{-6}$ Torr) to reduce the effect of residual gases before introducing the Ar gas into the process chamber. Before film deposition, the graphite target was sputter cleaned for 3-10 min, depending on the previous time of exposure of the chamber to the atmosphere, and the Si(100) substrate was sputter etched for 3 min to remove the native oxide layer. The precleaning process was carried out at 250 W forward rf power, 3 mTorr working pressure, and 20 sccm argon gas flow rate. All the a-C films were synthesized under 3 mTorr working pressure and 20 sccm gas flow rate. The substrate temperature was maintained at room temperature by a cooling system. Film depositions were performed at five different combinations of forward rf power P_f, substrate bias voltage V_S, and deposition time t: (i) 200 W $\leq P_f \leq$ 750 W, V_S = -200 V, t = 3 min; (ii) P_f = 750 W, 0 V $\geq V_S \geq$ -300 V, t = 3 min; (iii) P_f = 200 W, 0 V $\geq V_S \geq$ -300 V, t = 3 min; (iv) P_f = 750 W, V_S = -200 V, 2 min $\leq t \leq$ 11 min; (v) P_f = 200 W, V_S = -200 V, 2 min $\leq t \leq$ 11 min. Hereafter, films produced under these deposition parameters will be referred to group I through V, respectively.

The film thickness t_f was measured directly from cross-sectional images obtained by a high-resolution TEM (Philips CM300FEG/UT) with the instrumental resolution equal to 1.7 Å. The wafer thickness t_s was measured with a probe instrument (Millitron), while the wafer curvature

radius was determined before and after film deposition by laser scanning (Flexus). The average residual stress σ_r in the films was determined using Stoney equation (Brenner et al., 1949):

$$\sigma_r = \left(\frac{e}{1-\nu}\right)_s \frac{t_s^2}{6t_f}\left(\frac{1}{r} - \frac{1}{r_o}\right),\tag{1}$$

where $\left(\dfrac{E}{1-\nu}\right)_s$ is the biaxial modulus of the Si(100) substrate (assumed equal to 180.5 GPa (Brantley, 1973)), and r_o and r are the wafer curvature radii before and after film deposition, respectively. Based on energy balance consideration, the Ar^+ impinging flux J_{Ar^+} is given by

$$J_{Ar^+} = \frac{P_a}{eA(2V_p - V_T - V_S)},\tag{2}$$

where e is the electron charge, V_p is the time-average plasma bulk voltage (≈ 10 V), V_T and V_S are the time-average voltages at the target and substrate surfaces, respectively, P_a is the absorbed rf power, and A (= 324 cm^2) is the electrode area. $A = 324\,\text{cm}^2$ for present sputtering system. Table I gives the thickness and residual stress in each film in terms of the corresponding deposition conditions.

III RESULTS AND DISCUSSION

A. Experimental results

The compressive residual stress in rf sputtered a-C films strongly depends on the deposition conditions. It will be shown that the Ar^+ bombardment on the growing film surface controls the magnitude of the residual stress. The Ar^+ bombardment effect depends on the Ar^+ kinetic energy E_{Ar^+}, impinging Ar^+ flux J_{Ar^+} and bombardment (deposition) time t.

Fig. 1 shows the effect of the Ar^+ impinging flux J_{Ar^+} on the residual stress in the a-C films of group I. Both Ar^+ kinetic energy E_{Ar^+} and bombardment time t were fixed at 210 eV ($V_S =$ -200 V) and 3 min, respectively, in this group of film depositions. It can be seen that the enhancement of the Ar^+ bombardment effect due to the increase of the Ar^+ impinging flux J_{Ar^+} resulted in the linear increase of the compressive residual stress from 2.36 to 5.89 GPa.

Fig. 2 shows the dependence of the residual stress on the Ar^+ kinetic energy E_{Ar^+} of a-C films (group II and III). The Ar^+ impinging flux J_{Ar^+} during film growth in group II and III were fixed at $\sim 8.2 \times 10^{19}$ and $\sim 4.5 \times 10^{19}$ ions/m²·s, respectively (Table I). In both groups, the bombardment time t during film growth was equal to 3 min. In the absence of Ar^+ bombarding during film growth, the compressive residual stress ($\sim$ 0.8 GPa) was independent of the forward rf power. However, the dependence of the evolution of the compressive residual stress on the Ar^+ kinetic energy E_{Ar^+} and impinging flux J_{Ar^+} was complex. The compressive residual stress in the a-C films deposited under $P_f =$ 750 W (group II) increased first from 0.75 to 6.77 GPa with the increase of the Ar^+ kinetic energy E_{Ar^+} from 10 to 160 eV, and then decreased slightly to 5.89 GPa for $E_{Ar^+} >$ 160 eV, reaching a steady-state of $\sim$ 6 GPa. Although the compressive residual stress in the a-C films deposited under $P_f =$ 200 W (group III) also increased initially from 0.83 to 4.83 GPa with the increase of Ar^+ kinetic energy E_{Ar^+} from 10 to 60 eV, it decreased continuously for $E_{Ar^+} >$ 60 eV, indicating the occurrence of stress relaxation. The possible stress relaxation mechanisms are thermal spike processes (Davis, 1993) and interfacial tension effect. These mechanisms will be discussed in detail later.

Fig. 3 shows the effect of the bombarding time on the compressive residual stress in the a-C films synthesized under P_f = 750 W (group IV) and P_f = 200 W (group V). The Ar$^+$ kinetic energy E_{Ar^+} was fixed at 210 eV (V_S = -200 V) during the film deposition, while the Ar$^+$ impinging flux J_{Ar^+} during the growth of a-C films in group IV and V was fixed at ~8.2×10^{19} and ~4.8×10^{19} ions/m^2·s (Table I). The compressive residual stress in the a-C films of group IV increased initially from 5.89 to 11.44 GPa with the increase of the Ar$^+$ bombardment time, and later decreased slightly to a steady-state value of ~ 9.6 GPa. However, the compressive residual stress in the a-C films of group V increased monotonically from 2.36 GPa to a steady-state of ~ 4 GPa.

B. Kinetic energy of sputtered carbon atoms

From the experimental results mentioned above, it is found that Ar$^+$ bombardment had a significant effect on the compressive residual stress in rf sputtered a-C films. Carbon atoms ejected from the graphite target also gained kinetic energy from the Ar$^+$ sputtering process. The kinetic energy effect of carbon atoms condensing at the film surface on the residual stress requires further examination. The kinetic energy of the carbon atoms condensing at the film surface is a function of the kinetic energy of the carbon atoms ejected from the target and the chamber pressure.

Thompson (1968) proposed a model to describe the energy distribution of sputtered atoms from the target, which yields the following relationship:

$$\frac{dN_E}{N} = \frac{1 - \left(\frac{(M_1 + M_2)^2 (E_B + E)}{4 M_1 M_2 E_{ion}} \right)^{1/2}}{E^2 (1 + \frac{E_B}{E})^3}, \tag{3}$$

where N is the total number of atoms ejected from the target, dN_E is the number of atoms ejected from the target with kinetic energy in the range of E and $E + dE$, M_1 and M_2 are the masses of the target atoms and incident ions, respectively, E_{ion} is the kinetic energy of incident ions, and E_B is the target surface binding energy. For graphite, E_B = 3.5 eV (Lifshitz et al., 1990). The kinetic energy E_{Ar^+} of incident Ar^+ can be obtained from the target self-bias voltage. For rf sputtered a-C films synthesized under conditions of 750 W forward rf power and zero substrate bias, the kinetic energy E_{Ar^+} of Ar^+ impinging on the target surface was ~1755 eV (Table I). The kinetic energy distributions of carbon atoms ejected from the target surface is calculated from Eq. (3) and shown in Fig. 4. The average kinetic energy of carbon atoms calculated from this energy distribution is 24.4 eV.

The kinetic energy of carbon atoms ejected from the graphite target by Ar^+ bombardment decreases progressively during travel across the target-substrate space due to scattering mainly by the Ar gas. As shown below, the energy ratio r of a sputtered atom before and after one scattering event is given by (Westwood, 1978)

$$r = \frac{<E_0>}{<E_1>} = e^\omega, \tag{4}$$

where $<E_0>$ and $<E_1>$ are the kinetic energies of a sputtered atom before and after scattering, respectively, and parameter ω is given by (Westwood, 1978)

$$\omega = \frac{(\alpha - 1)^2}{2\alpha} \ln(\frac{\alpha + 1}{\alpha - 1}) - 1, \tag{5}$$

where α is the mass ratio of the sputtering gas atom to the sputtered atom. For a sputtered carbon atom scattered by Ar gas, ω = -0.494 and r = 0.6099.

The average distance L traveled by a sputtered carbon atom after its *nth* scattering event is given by (Westwood, 1978)

$$L = n\lambda\sqrt{2}\cos(\frac{<\theta>}{2}),\tag{6}$$

where $<\theta>$ is the spatial average of the scatter angle of carbon atoms due to collisions with Ar atoms, which for carbon-argon system is 78.46°; λ is the mean free path of a sputtered carbon atom traveling through the target-substrate space, given by

$$\lambda = 2.2/p \text{ (cm)},\tag{7}$$

where p is the working pressure in Pa. Therefore, the ratio R_n of the kinetic energy of a carbon atom before and after n scatterings is given by

$$R_n = \exp(n\omega) = \exp(-0.205\,pL).\tag{8}$$

In the present sputtering system, the distance L between the target and the substrate was 7 cm, and the working pressure was set at 3 mTorr (0.4 Pa) during film growth. Hence, $R_n = 0.56$, and the average kinetic energy of carbon atoms condensing at the film surface was approximately equal to 56% of the average kinetic energy of carbon atoms ejected from the target (i.e., 13.7 eV).

The average kinetic energy of sputtered carbon atoms condensing at the film surface was comparable to that of Ar^+ bombarding the film surface (~10 eV) when the substrate was not negatively biased. However, the impinging flux of sputtered carbon atoms was much smaller than that of Ar^+ and the direction of carbon atoms ejected from the target surface was random. Therefore, the compressive residual stress in the film was predominantly affected by the Ar^+ bombardment, while the carbon atom striking effect was secondary.

C. Effect of Ar^+ Bombardment

In the absence of substrate biasing, the kinetic energy (~10 eV) of Ar^+ striking the film surface was independent of the rf power and too low to produce a significant bombardment effect. Therefore, the compressive residual stress in the film was independent of the rf power (Fig. 2). However, the effect of Ar^+ bombardment on the compressive residual stress became significant when the substrate was biased negatively during film growth.

As reported previously, the experimental results showed that the compressive residual stress in sputtered a-C films increased with the Ar^+ impinging flux J_{Ar^+} on the film surface, and depended on the Ar^+ kinetic energy E_{Ar^+}. D'Heurle (1970) attributed the origin of a compressive residual stresses in sputtered films to "shot-peening" of energetic particles arriving at the film surface at significant kinetic energy. Since then different models have been proposed for the ion-peening process (Hoffman et al., 1980; Windischmann, 1987). Windischmann (1987, 1992) used ballistic atomic collisional descriptions to develop a theoretical model that explains the origin of the compressive residual stresses in sputtered films based on the following assumptions: (i) a volumetric distortion is produced due to the displacement of n atoms per unit volume from their equilibrium positions through a series of primary and recoil collisions, (ii) the volumetric distortion is frozen in place due to insignificant mass transport and defect mobility at low deposition temperatures ($T/T_m < 0.25$, where T is the deposition temperature and T_m is the melting temperature), and (iii) the relative volumetric distortion (strain) is proportional to the fractional number of atoms n/N displaced from their equilibrium positions, where N is the atomic number density of sputtered atoms condensing on the film surface. Therefore, the compressive residual stress in sputtered film is given by (Windischmann, 1987, 1992)

$$\sigma_r = \left(\frac{E}{1-v}\right)_f \left(\frac{Kn}{N}\right), \tag{9}$$

where $\left(\dfrac{E}{1-v}\right)_f$ is the biaxial modulus of the sputtered film, and K is a proportionality factor. Based on the knock-on linear cascade theory of sputtering (Sigmund, 1981), the number of atoms per unit volume n displaced due to the bombardment effect can be obtained as the product of the forward sputtering yield γ and the ion flux J_{Ar^+} as for the carbon-argon system

$$n = J_{Ar^+}\gamma . \qquad (10)$$

Neglecting the effect of the carbon atom striking at the film surface, the compressive residual stress in the sputtered a-C films can be expressed as (Mounier et al., 1996)

$$\sigma_r = 13.36\left(\frac{E}{1-v}\right)_f \left(\frac{K}{N}\right)\frac{E_{Ar^+}^{1/2}}{U_o} J_{Ar^+}, \qquad (11)$$

where U_0 is the sublimation energy of carbon.

According to Eq. (11), the compressive residual stress increases linearly with the Ar^+ impinging flux. The experimental data reported earlier in this study are in agreement with Eq. (11) (Fig. 1). However, the compressive residual stress always increases with the Ar^+ kinetic energy E_{Ar^+} according to Eq. (11) conversely to the results shown in Fig. 2. As mentioned previously, the relationship between σ_r and E_{Ar^+} is complex due to stress relaxation during the film growth. The possible mechanisms controlling stress relaxation are thermal spike processes and interfacial tension effect.

The effect of Ar^+ bombardment also depends on the film thickness. The plasma sheath behavior plays an important role in the rf sputtered a-C film growth. The plasma sheaths in low-pressure rf discharge can be modeled as pure capacitors C_s when $\omega\tau_i \gg 1$, where ω is the frequency of the applied field and τ_i is the ion transit time through the sheath. The growing a-C

film and the substrate form a capacitor $C_{f,s}$ because the a-C film is a dielectric material. Fig. 5 shows the equivalent electrical circuit of a single rf power sputtering system. The substrate bias voltage V_S is distributed in the film-substrate capacitor $C_{f,s}$ and the capacitor of the plasma sheath near the substrate C_s. The Ar$^+$ kinetic energy E_{Ar^+} is determined by the potential V_{sf} between the sheath edge and the growing a-C film surface. Using the simple electrical analog shown in Fig. 5, the potential V_{sf} can be expressed by

$$V_{sf} = \frac{C_T}{C_s} V, \tag{12}$$

where $C_T = \dfrac{C_s C_{f,s}}{C_s + C_{f,s}}$, $C_s = \dfrac{\varepsilon_s \varepsilon_o}{d_s}$, $C_{f,s} = \dfrac{\varepsilon_f \varepsilon_o}{t_f}$, $V = V_P - V_S$, ε_0 is the electrical permittivity in vacuum, ε_s and ε_f are the dielectric constants of the plasma sheath and the a-C film, respectively, and d_s is the thickness of the plasma sheath near the substrate. For rf discharge conditions of 3 mTorr working pressure, 300 K environmental temperature, ~750 W absorbed rf power and 7 cm spacing between the target and substrate, d_s is estimated to be about ~360 μm using Child Law, and ε_s is given by (Lieberman et al., 1994)

$$\varepsilon_s = \frac{en_0 L}{V} \frac{d_s}{\varepsilon_0}, \tag{13}$$

where n_0 is the plasma density, which is a function of the absorbed rf power P_a.

Fig. 6 shows the variation of the potential V_{sf} with the film thickness for rf discharge conditions of 740 W absorbed rf power and -200 V substrate bias voltage. The kinetic energy E_{Ar^+} decreases continuously with film growth, hence, decreasing the effect of Ar$^+$ bombardment. The compressive residual stress in the a-C films of group IV increased initially with the deposition

time from 5.89 to 11.44 GPa, and then decreased slightly when the film thickness above 70 nm, and eventually reaching a steady-state of ~9.6 GPa (Fig. 3) due to the decrease of E_{Ar^+} from 210 eV to less than 180 eV (Fig. 6).

D. Thermal spike effect

As mentioned previously, the prediction based on the Windischmann model that the compressive residual stress always increases with E_{Ar^+} predicted is not supported by the experiments (Fig. 2). Stress relaxation can occur during film growth. Davis (1993) proposed a model that takes into account the thermal spike effect to explain stress relaxation in a growing film. The carbon atoms displaced due to the knock-on process by both the energetic Ar^+ and the implanted energetic carbon atoms are responsible for the development of the compressive residual stress in the sputtered a-C films (Windischmann, 1987, 1992). However, because the implanted carbon atoms are metastable, they can escape to the film surface if they acquire sufficient excitation energy E_0. The kinetic energy of bombarding particles can be transferred to the film atoms by cascade collisions over a very short impact range. The resulting intense local heating (thermal spike effect) provides energy to the metastable atoms in the film to migrate to the surface.

Assuming that each implanted carbon atom receiving energy greater than E_0 migrates to the film surface and considering that a steady-state is reached between implantation and relaxation processes, the rate difference $n_i - n_r$ is constant, given by (Davis, 1993)

$$n_i - n_r = R \frac{n}{N}, \tag{14}$$

where n_i and n_r are the implantation rate of carbon atoms per unit area and the migration rate of carbon atoms per unit area, respectively; R is the constant steady-state rate per unit area at which

implanted carbon atoms are incorporated into the film. Therefore, the compressive residual stress

in sputtered a-C films can be obtained by (Davis, 1993)

$$\sigma_r = K \left(\frac{E}{1-v} \right)_f \frac{13.36}{U_o} \frac{J_{Ar^+} E_{Ar^+}^{1/2}}{R + 0.016\rho \left(\frac{E_{Ar^+}}{E_o} \right)^{5/3} J_{Ar^+}}. \tag{15}$$

In Eq. (15), K, $\left(\frac{E}{1-v} \right)_f$, U_0, and ρ are constant, while R, J_{Ar^+}, and E_{Ar^+} depend on the

deposition conditions. When $R \gg 0.016\rho \left(\frac{E_{Ar^+}}{E_0} \right)^{5/3} J_{Ar^+}$, carbon atom implantation is dominant

and, hence, $\sigma_r \propto J_{Ar^+} E_{Ar^+}^{1/2}$. However, when $R \ll 0.016\rho \left(\frac{E_{Ar^+}}{E_0} \right)^{5/3} J_{Ar^+}$, carbon atom migration

to the film surface is the dominant process and, thus, $\sigma_r \propto E_{Ar^+}^{-7/6}$ (stress relaxation). This explains

why the compressive residual stress in the a-C films of group III decreased continuously from 4.83

to 2.36 GPa when $E_{Ar^+} > 60$ eV (Fig. 2).

The compressive residual stress in the a-C films of group II was also relaxed due to the

thermal spike effect. However, the stress relaxation was weaker than that in the a-C films of group

III (Fig. 2). The possible reason for this difference is the film thickness dependence of the thermal

spike effect. In low-pressure rf sputtering deposition, Ar^+ bombardment on the growing a-C film

surface causes cascade collisions between carbon atoms, which diminishes at a characteristic depth

Λ below the film surface, defined as the impact depth. Since most of the recoil carbon atoms move

only within the impact region, the depth Λ affects the magnitude of the residual stress. This

phenomenon is shown schematically in Fig. 7. When the film thickness is less than the impact

depth ($t_f < \Lambda$), the recoil carbon atoms can only migrate to the film surface because it is more

difficult to penetrate the single crystal Si(100) substrate (Fig. 7 a). This process results in significant relaxation of the compressive residual stress in the film. This is the case in the present films discussed above. When the film thickness exceeds the impact depth ($t_f > \Lambda$), some of the recoil carbon atoms can migrate into the bulk of the film resulting in film densification and a decrease of thermal spike effect on stress relaxation (Fig. 7 b) This explains the less pronounced stress relaxation in the *a*-C films of group III (Fig. 2).

E.   Interfacial tension effect

A thin interfacial layer was formed during the initial stage of *a*-C film growth by rf sputtering. Davis et al. (1995) observed the formation of a 5-nm-thick interfacial layer in *ta*-C films deposited by filtered cathodic arc apparatus using a transmission electron microscope. Logothetidis et al. (2001) studied real- time growth of *a*-C films deposited by sputtering using *in-situ* ellipsometer, and observed a two-stage growth process. In the initial stage of film nucleation and coalescence encountered up to a film thickness of ~5 nm, the film growth rate was low, compared to the film growth rate at a later stage. Cross-sectional images of the rf sputtered *a*-C films of this study obtained with a high-resolution TEM (Philips CM300FEG/UT) reveal the existence of a ~37-Å-thick interfacial layer between the *a*-C films and the Si(100) substrate (Fig. 8). It is believed that the interfacial layer enhances the adhesion of the *a*-C film to the Si(100) substrate and relaxes the compressive residual stress (Kelires et al., 1999). During the initial stage of *a*-C film growth, the bond lengths of carbon atoms must accommodate those of silicon atoms in the outermost layer of the substrate. Thus, due to the lattice mismatch, a tensile residual stress evolves in the interfacial layer and, the thinner the film, the larger the effect of the tensile stress in the interfacial layer. As the film thickness increases above ~7 - 8 Å, a compressive stress develops progressively in the film because the tensile stress in the interfacial layer is exceeded by the compressive stress in the

growing film generated by implanted atoms through the knock-on process (Windischmann 1987, 1992). Therefore, compressive stress relaxation due to the tensile stress in the interfacial layer can only be observed with ultrathin films. The a-C films of group V are less than 20 nm in thickness (Table I). The thickness of the first two samples is 36 Å and 56 Å, respectively. Considering that the thickness of the interfacial layer is ~37 Å in all cases, the compressive residual stress in these two a-C films of 2.72 and 2.36 GPa, respectively, represents the compressive stress in the interfacial layer. With the increase of the deposition time, the compressive residual stress attains a steady-state of ~4 GPa (Fig. 3 and Table I). The relatively low compressive residual stress is attributed to the counter effect of the tensile stress in the interfacial layer. This stress relaxation effect due to the interfacial tensile stress is not observed in the a-C films of group IV (Fig. 3) due to the large thickness of these films (Table I).

IV   CONCLUSIONS

In this study, the development of a compressive residual stress in rf sputtered a-C films was examined in light of stress measurement and results from an analysis of the effects of the Ar^+ bombardment, thermal spike process, and tensile stress in the interfacial layer. It was shown that the residual stress was essentially affected by the Ar^+ kinetic energy, impinging flux, and energetic particle bombardment time on the growing film surface. However, in the absence of Ar^+ bombardment (zero substrate bias voltage) the relatively low compressive residual stress (~0.8 GPa) was found to be independent of the Ar^+ impinging flux. It was also shown that carbon atom impingement was secondary compared to that of Ar^+ bombardment. A high compressive residual stress (~10 GPa) was produced with intensive Ar^+ bombardment on the growing a-C films. The origins and evolution of the compressive residual stress were explained in terms of Ar^+

bombardment. A film thickness dependence of the Ar^+ bombardment effect was observed for relatively thick a-C films (i.e., $t_f > 70$ nm). The compressive residual stress in rf sputtered a-C film can be relaxed by either thermal spike processes or the tension stress arising in the ~37-Å-thick interfacial layer bonding the a-C film to the Si(100) substrate.

ACKNOWLEDGEMENTS

REFERENCES

E. Mounier, P. Juliet, E. Quesnel and Y. Pauleau, Surf. Coating Technol., **77**, 548 (1995).

E. Mounier, and Y. Pauleau, Diamond and Related Mater., **6**, 1182 (1997).

D. A. Hills and D. W. Ashelby, wear, **75**, 221 (1982).

N. Ye, Ch. 5 in *Contact Mechanics of Elastic-Plastic Layered Media With Smooth and Rough Surfaces* (*Dissertation*) (UC, Berkeley, 2002).

H. Windischmann, Crit. Rev. Solid State Mater. Sci. **17**, 547 (1992).

C. A. Davis, Thin Solid Films **226**, 30 (1993).

E. S. Machlin, *Materials Science in Microelectronics, The Relationships between Thin Film Processing and Structure* (Giro Press, Croton-on-Hudson, New York, 1995).

W. D. Nix, Metall. Trans. A, **20A** 1989 (1989).

W. Lu and K. Komvopoulos, Appl. Phys. Lett., **76**, 3206 (2000).

A. Brenner and S. Senderoff, J. Res. Natl. Bur., **42**, 105 (1949).

M. W. Thompson, Philos. Mag., **18**, 377 (1968).

Y. Lifshitz, S. R. Kasi, J. W. Rabalais and W. Eckstein, Phys. Rev. B, **41**, 10468 (1990).

W. D. Westwood, J. Vac. Sci. Thechnol., **15**, 1 (1978).

F. M. D'Heurle, Metall. Trans., **1**, 725 (1970).

D. W. Hoffman and M. R. Gaertner, J. Vac. Sci. Thechnol., **17**, 425 (1980).

H. Windischmann, J. Appl. Phys., **62**, 1800 (1987).

P. Sigmund, Ch. 2 in *Sputtering by Particle Bombardment I*, edited by R. Behrisch (Springer, Berlin, 1981).

E. Mounier and Y. Pauleau, J. Vac. Sci. Thechnol. A, **14**, 2535 (1996).

M. A. Lieberman and A. J. Lichtenberg, *Principles of Plasma Discharges and Materials Processing* (Wiley, New York, 1994).

C. A. Davis, K. M. Knowles and G. A. J. Amaratunga, Surf. Coatings Technol., **76-77**, 316 (1995).

S. Logothetidis, M. Gioti and P. Patsalas, Diamond and Related Mater., **10**, 117 (2001).

P. C. Kelires, M. Gioti and S. Logothetidis, Phys. Rev. B, **59**, 5074 (1999).

Table I   Thickness and compressive residual stresses

Group	Forward rf power (W)	Absorbed rf power (W)	Substrate bias (V)	Target bias (V)	Ion flux (x 10^{19} ions/m^2-s)	Deposition time (min)	Thickness (nm)	stress (GPa)
I	200	172.5	-200	-499	4.68	3	5.6	-2.36
	300	285	-200	-790	5.48	3	10.9	-3.1
	400	388	-200	-1000	6.17	3	15.6	-4.26
	500	500	-200	-1199	6.83	3	18.9	-4.75
	600	600	-200	-1340	7.45	3	23.1	-4.92
	750	746	-200	-1550	8.16	3	28.7	-5.89
II	750	715	-300	-1345	8.32	3	26.6	-6.22
	750	745.5	-150	-1600	8.15	3	29.6	-6.77
	750	747.5	-100	-1630	8.27	3	30.8	-6.14
	750	746.5	-50	-1685	8.23	3	32.2	-4.53
	750	741.5	0	-1745	8.13	3	34.1	-0.75
III	200	188	-150	-650	4.47	3	7.2	-4.11
	200	196.5	-100	-730	4.5	3	8.5	-4.5
	200	197.5	-50	-795	4.45	3	9.2	-4.83
	200	198	0	-885	4.26	3	9.8	-0.83

Table I   Thickness and compressive residual stresses (Cont'd)

Group	Forward rf power (W)	Absorbed rf power (W)	Substrate bias (V)	Target bias (V)	Ion flux (x 10^{19} ions/m^2-s)	Deposition time (min)	Thickness (nm)	stress (GPa)
IV	750	747	-200	-1540	8.22	5	48.6	-8.66
	750	748	-200	-1540	8.23	7	67.8	-11.4
	750	746	-200	-1550	8.16	9	87	-9.78
	750	745	-200	-1555	8.12	11	106.5	-9.55
V	200	180	-200	-500	4.88	2	3.6	-2.72
	200	172.5	-200	-499	4.68	3	5.6	-2.36
	200	176	-200	-499	4.78	5	8.8	-3.86
	200	180	-200	-500	4.88	7	12.7	-3.64
	200	178	-200	-500	4.83	9	16.1	-4.27
	200	179	-200	-499	4.86	11	19.8	-3.89
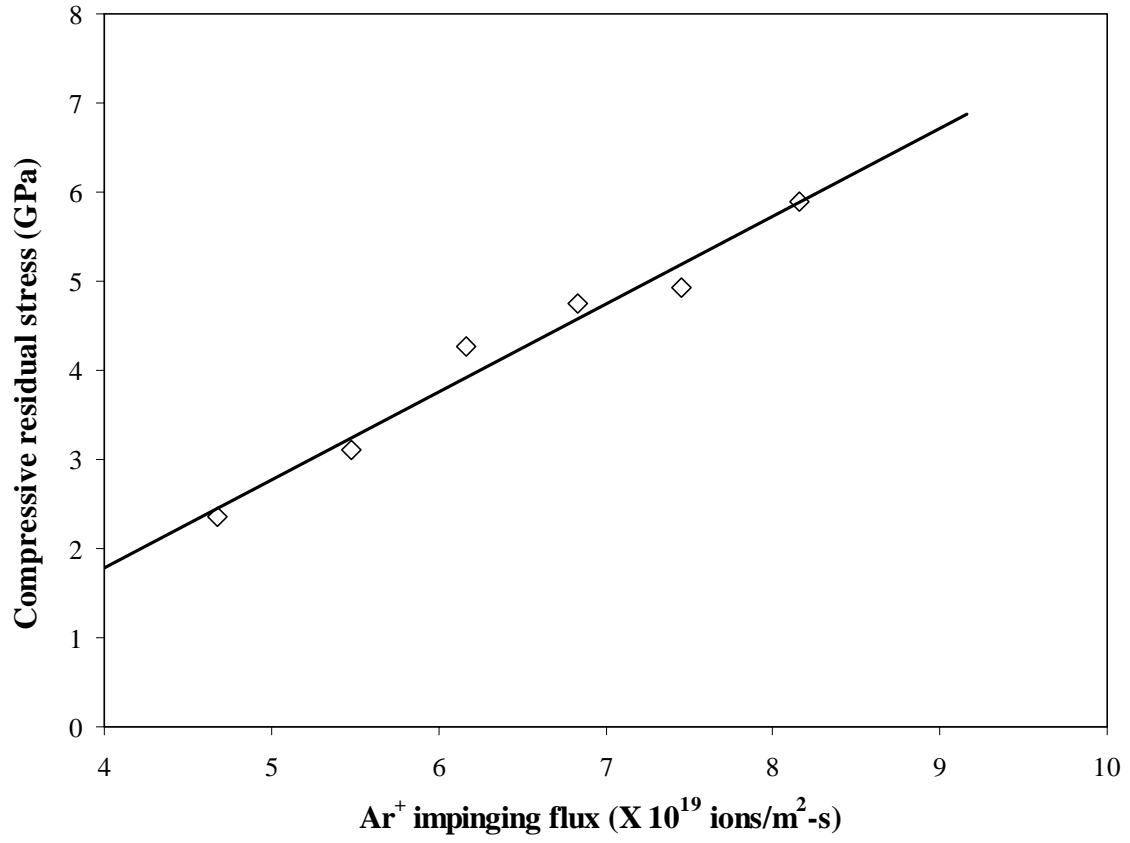
Figure 1   Effect of Ar$^+$ impinging flux J_{Ar^+} on compressive residual stress in sputtered a-C films synthesized under conditions of -200 V substrate bias, 3 mTorr working pressure, 20 sccm gas flow rate, and 3 minutes deposition time (Group I).
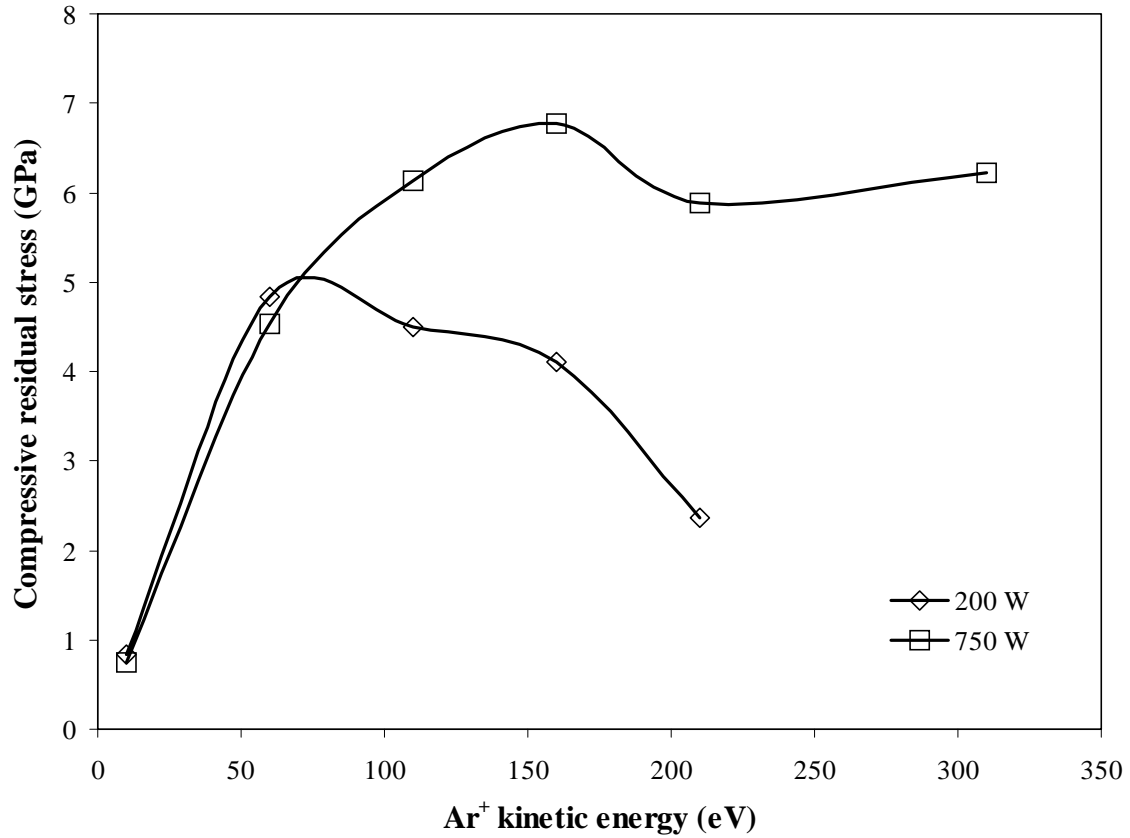
Figure 2   Effect of Ar$^+$ kinetic energy E_{Ar^+} on compressive residual stress in the *a*-C films synthesized under conditions of 750 W (group II) and 200 W (group III) forward rf power, 3 mTorr working pressure, 20 sccm gas flow rate, and 3 minutes deposition time.
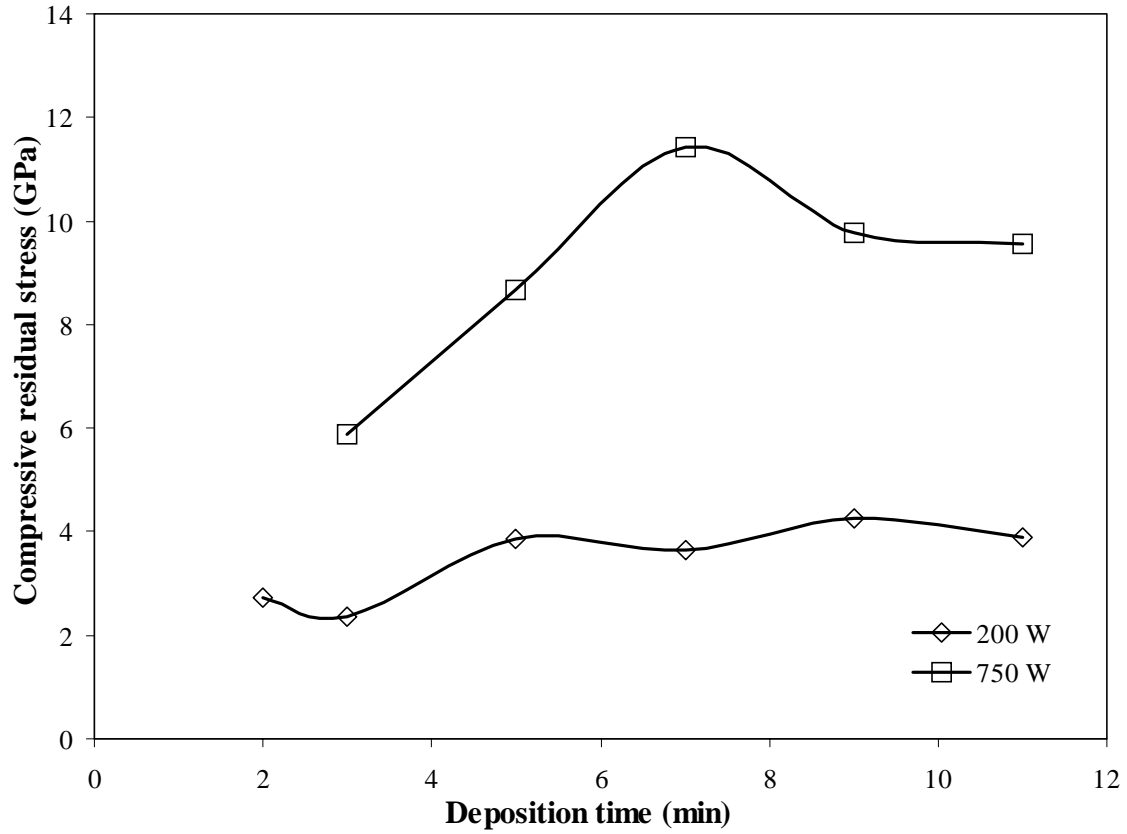
Figure 3   Effect of Ar$^+$ bombardment time t on compressive residual stress in the a-C films synthesized under conditions of 750 W (group IV) and 200 W (group V) forward rf power, 3 mTorr working pressure, 20 sccm gas flow rate, and deposition time varied between 2 and 11 minutes.
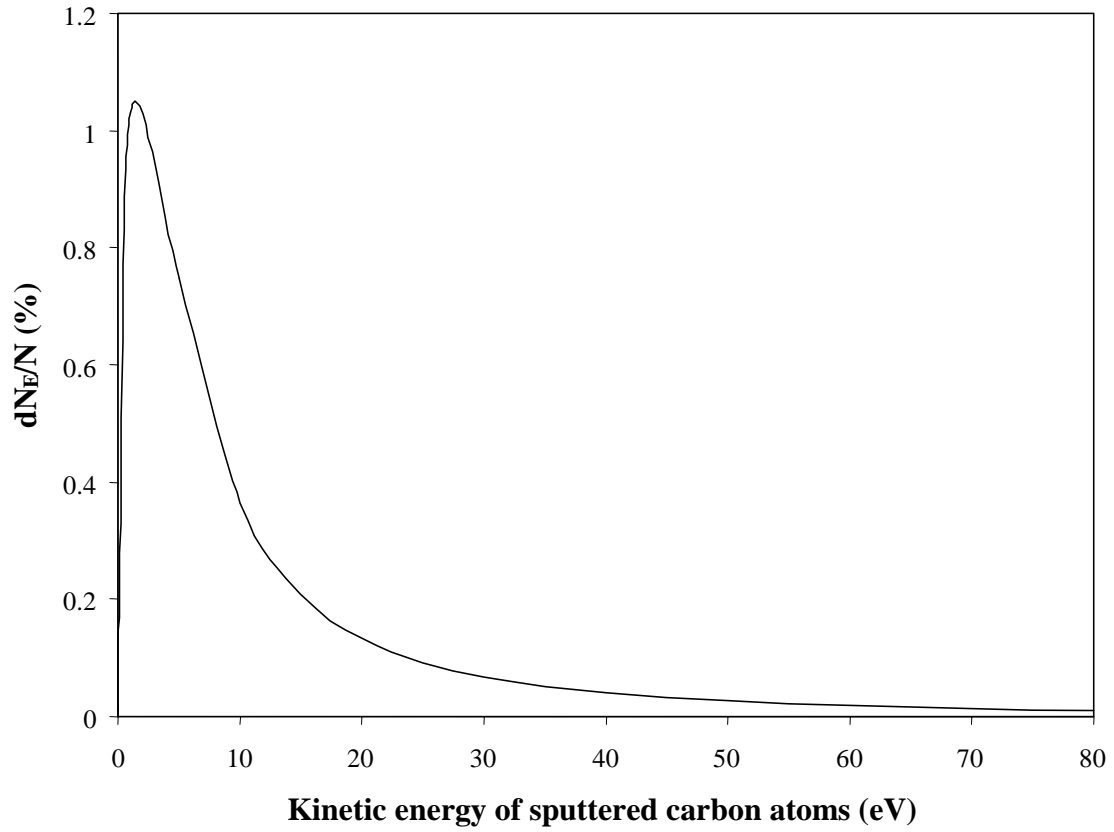
Figure 4   Distribution of kinetic energy of carbon atoms sputtered from the graphite target by Ar^+ sputtering of energy $E_{Ar^+} \approx 1755\,\mathrm{eV}$ obtained from Eq. (4-2).
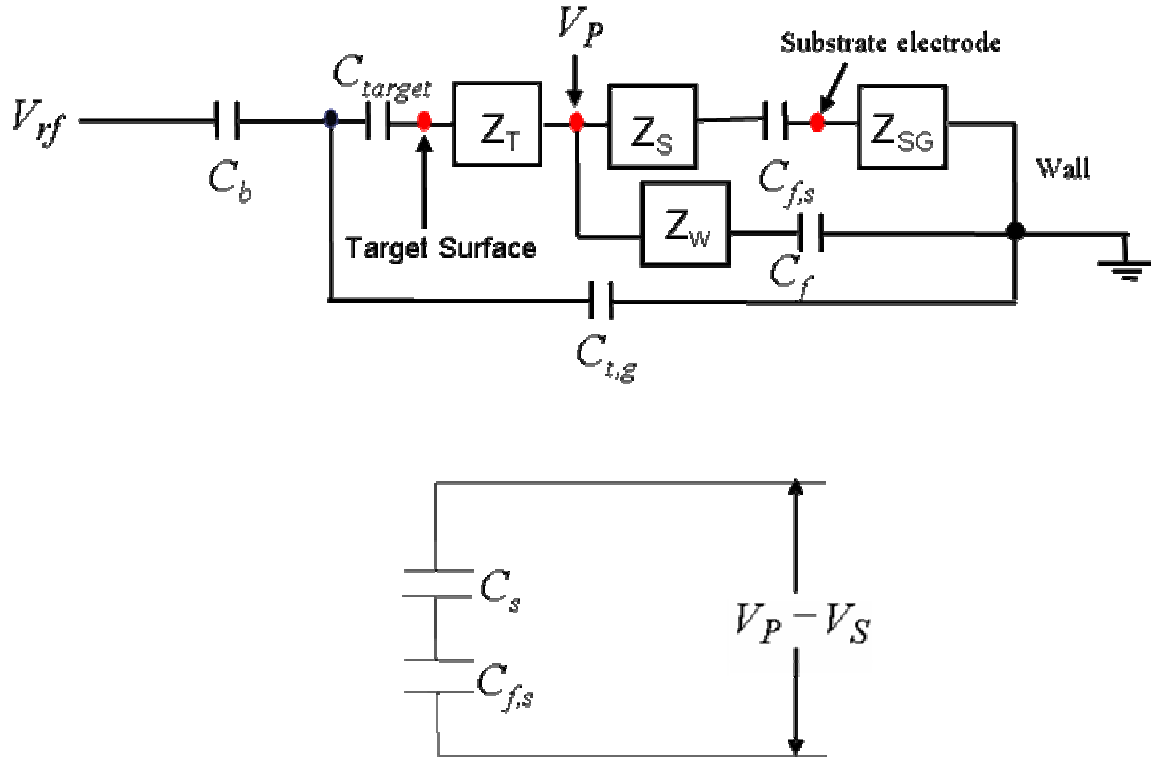
Figure 5   Equivalent electrical circuit of a single rf power sputtering system. Z_T, Z_S, and

Z_{SG} are impedances between target and plasma, between substrate and plasma,

between substrate and ground, respectively, and Z_W is the wall impedance.

C_b is the capacitance using to block dc current, C_s is the capacitance

of plasma sheath near the substrate, $C_{f,s}$ is the capacitance between a-

C film and substrate surface, C_{target} is the e capacitance of target, $C_{t,g}$

is the capacitance between target and ground, C_f is the capacitance

of thin film on the wall. V_P, V_S and V_{rf} : the potentials of bulk

plasma, substrate and rf power supply, respectively.
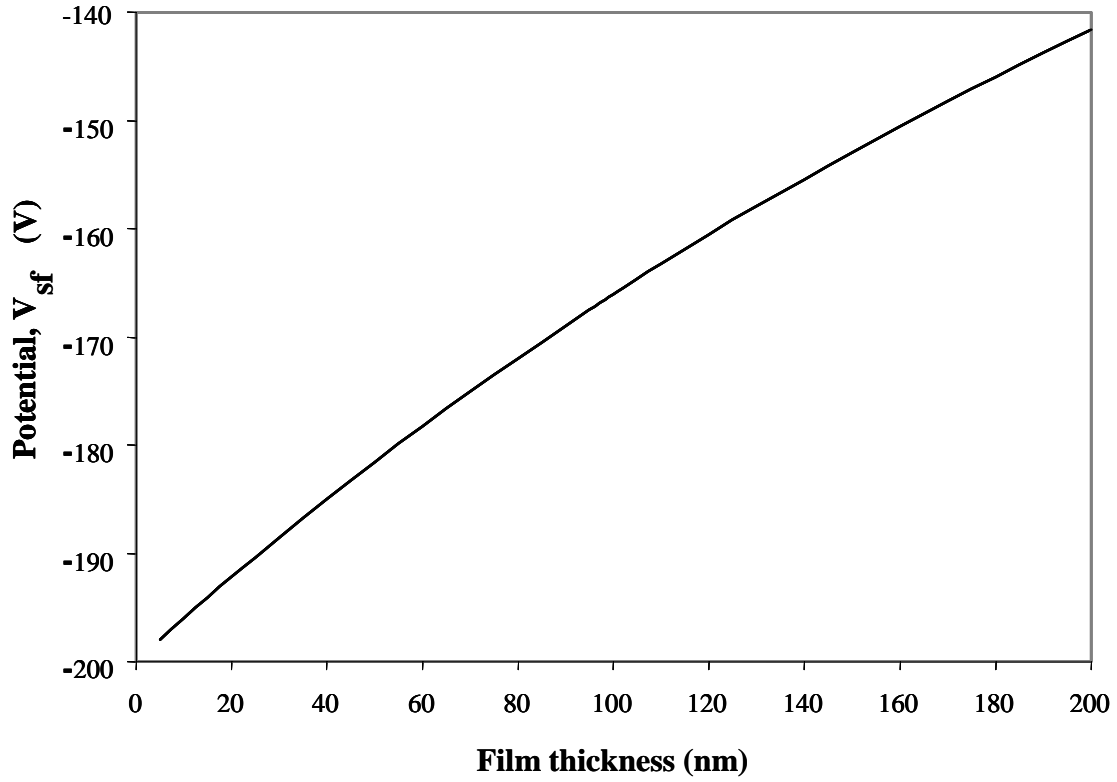
Figure 6   The potential V_{sf} between the plasma sheath edge near the substrate and the film surface versus film thickness.
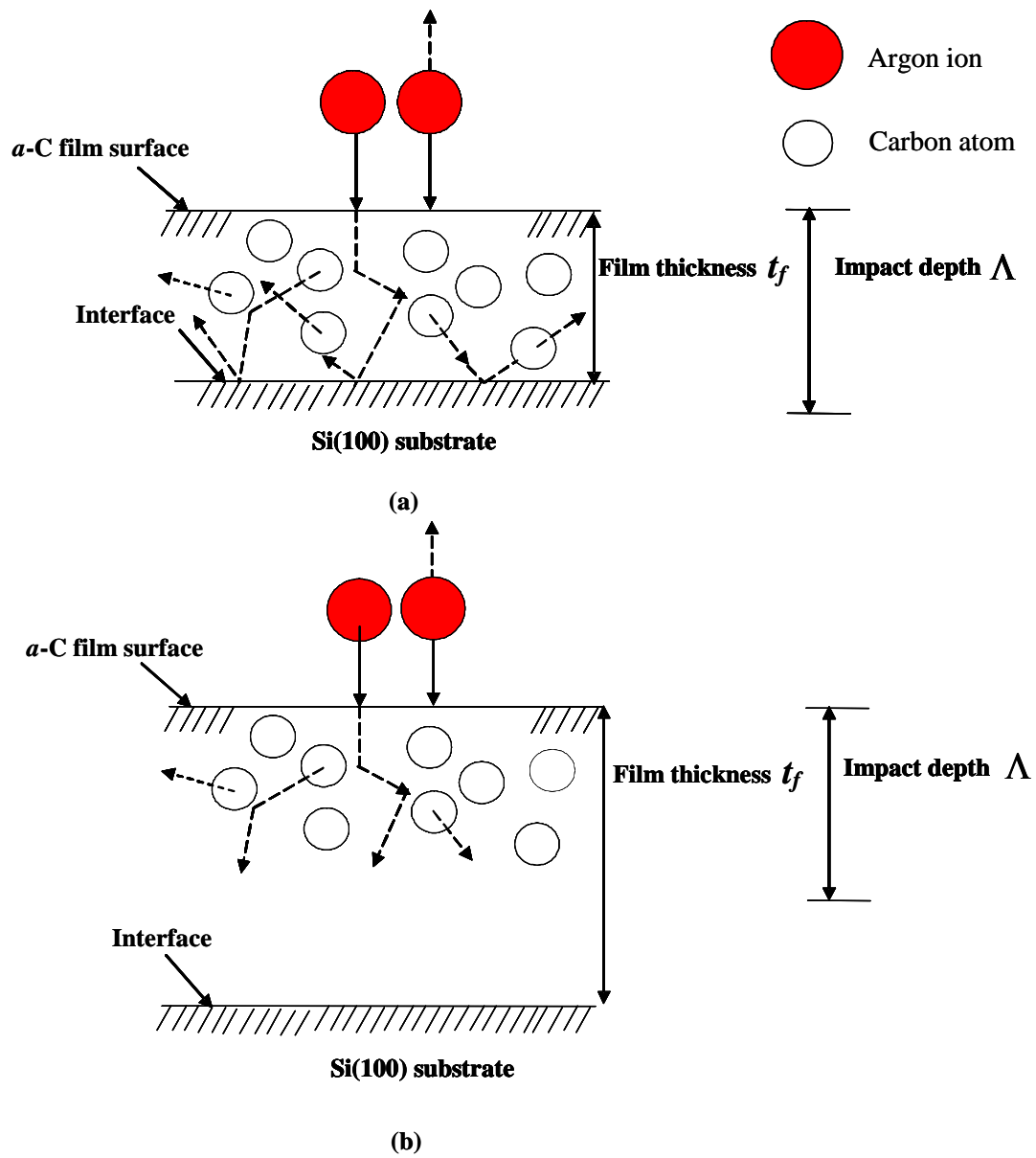
Figure 7   Film thickness dependence of the thermal spike effect.

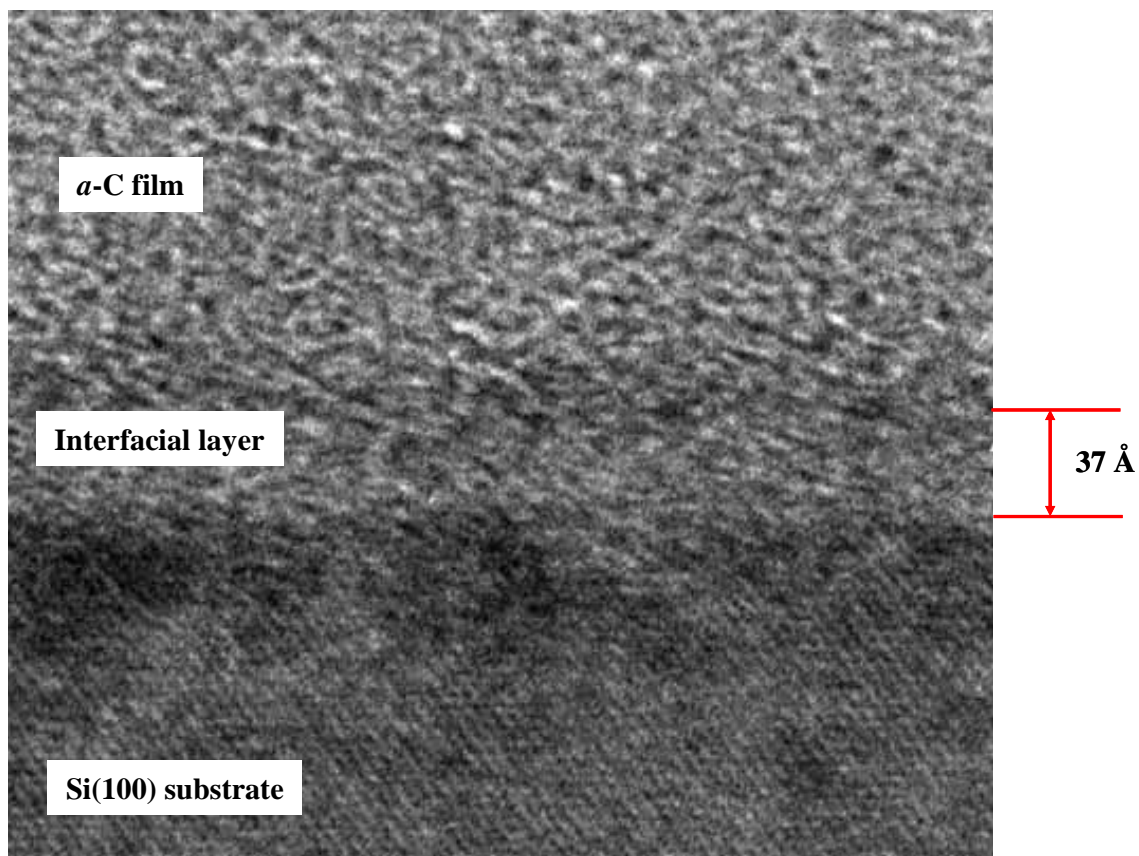a-C film

Interfacial layer

37 Å

Si(100) substrate

Figure 8   Cross-sectional transmission electron microscope image of rf sputtered *a*-C film deposited on Si(100) substrate under conditions of 750 W forward rf power, -200 V substrate bias voltage, 20 sccm gas flow rate, 3 mTorr working pressure, and 3 min deposition time.